Journal of Engineering and Applied Research (JEAR)

National University of Skills

Summer & Autumn 2025, Vol. 2, No. 2, p. 109- 120

Journal Homepage: https://jear.tvu.ac.ir

:10.48301/JEAR.2024.474745.1096

Feasibility Study of Manufacturing a Laparoscopic Stapler Joint Using Metal Injection Molding Process

Mahdi Aminian[1], Ramin Hashemi[2*], Amir Rasti[3], Ali Zeinolabedin-Beygi[4]

[1,2] School of Mechanical Engineering, Iran University of Science and Technology, Tehran, Iran
[3,4] Faculty of Mechanical Engineering, Tarbiat Modares University, Tehran, Iran

ARTICLE INFO

Article Type:
Original Research

Received: 02.22.2025
Revised: 05.25.2025
Accepted: 11.04.2025

Keyword:
Manufacturing
Feasibility
Metal injection molding
Laparoscopic Stapler
Feedstock

***Corresponding Author:**
Ramin Hashemi
Email:
rhashemi@iust.ac.ir

ABSTRACT

The metal powder injection process is a combination of powder metallurgy and plastic injection in the manufacturing field. This process has both the economic advantages of the plastic injection process and the mechanical properties of the powder metallurgy process; In such a way that a metal piece with desirable mechanical properties can be economically produced. Hence, this process has spread in various industries, including the medical equipment industry. The Metal Injection Molding (MIM) process can be divided into four parts: feedstock, injection molding, debinding and sintering. The metal powder is first combined with the polymer and injected into the mold, and then the polymer is destroyed in the debinding process, and the part is finalized in the sintering process. In this study, the joint part of the laparoscopic stapler was manufactured with the MIM process, and the details of all four parts of the process were explained for the desired part. After making the sample, it was concluded that the method is competitive with CNC machining and the main joint and Driver of the laparoscopic stapler can be made and produced with the same method.

E-ISSN: 3060-6357

Introduction

With advancements in science and technology, the need for advanced components made from new materials has increased. Modern manufacturing processes can greatly assist researchers in producing new parts required by various industries. For instance, materials capable of withstanding a wide range of temperatures can no longer be manufactured using traditional methods alone, necessitating the use of modern manufacturing techniques. Manufacturing processes are divided into four categories: welding [1], forming [2], casting [3] and machining [4]. One of the forming processes is powder metallurgy, which is used to manufacture metal and ceramic components. This method involves compressing powder as the raw material into the desired shape and then sintering it. The limitations of polymers in operating temperatures compared to metals and ceramics when using injection molding, along with the limitations of powder metallurgy in producing complex parts and its slow processing speed, led to the development of a new technique that integrates both processes. This technique, called Powder Injection Molding (PIM), enables the production of complex ceramic or metal parts in high volumes [5; 6]. PIM can be categorized into Ceramic Injection Molding (CIM) [7] and Metal Injection Molding (MIM) [8]. MIM is widely used in various industries, including automotive, defense, aerospace, electronics, and medical applications [9-11]. From an economic perspective, MIM is an efficient method for producing complex metal parts with near-net-shape geometry, significantly reducing the need for additional machining. This process is particularly suitable for manufacturing small components in large volumes, resulting in considerable cost savings [12]. Due to its capability to fabricate complex geometries with excellent mechanical properties and biocompatibility, MIM is widely applied in the production of surgical instruments, orthopedic implants, and minimally invasive device components. Studies have demonstrated that MIM-fabricated parts, especially those made from titanium and stainless steel alloys, meet stringent medical standards for mechanical strength and surface quality, making MIM a competitive alternative to traditional manufacturing methods in the medical industry [13;14].

In recent years, various studies have been conducted on this method due to the development of MIM processes [15-17]. Lin [18] manufactured a laptop hinge using MIM and demonstrated that an injection pressure of 1000 bar and an injection temperature of 160°C were optimal for molding the part with high fatigue resistance and strength. Shieddieque et al. [19] investigated the physical and mechanical properties of parts sintered at different temperatures (1300–1360°C) in both vacuum furnaces and argon-protected furnaces. Their results showed that porosity was higher in vacuum conditions than in argon gas, leading to lower density. The highest hardness was achieved with sintering at 1360°C for 1.5 hours under argon protection. Panahizadeh et al. [20] conducted experimental and numerical studies on MIM parameters and found that optimal values for injection speed, pressure, and

temperature were 60%, 60%, and 185°C, respectively. Hamidi et al. [21] investigated solvent debinding in the MIM process for 316L stainless steel. Their results showed that solvent removal at 60°C for 240 minutes was optimal as it effectively removed enough paraffin. Momeni and Alaei [22] optimized injection parameters in the MIM process for a steel component. They found that the optimal conditions for injecting feedstock containing low-alloy steel powder 4605 included an injection pressure of 133 bar, an injection temperature of 158°C, a mold temperature of 60°C, a holding time of 8 seconds, a holding pressure of 70 bar, a secondary holding time of 17 seconds, and an injection speed of 112 mm/s. Rezaei and Askari [23] studied optimal injection parameters for MIM in manufacturing a relatively complex part from a feedstock of low-alloy steel 4605, commonly used in industrial engines. They determined that an injection speed of 80 mm/s, an injection temperature of 155°C, a holding time of 9 seconds, a holding pressure of 83 bar, and an injection pressure of 132 bar were the optimal values for achieving maximum density. Yang et al. [24] showed that low injection temperatures for manufacturing parts made from a powder blend of alloy 6061 and 316L stainless steel in the MIM process resulted in voids and cracks, but increasing pressure and injection speed reduced these defects. Table 1 shows a comparative analysis of MIM and CNC machining for manufacturing components in medical applications.

Table 1. Comparative analysis of MIM and CNC machining for manufacturing components in medical applications

Parameter	MIM	Machining	Reference(s)
Roughness (Ra)	1.5–3.5 µm before polishing; <0.8 µm after finishing	0.4–1.6 µm	[4, 14]
Hardness (17-4PH)	280–320 Hv after sintering and aging	260–310 Hv, depending on cutting and heat treatment	[22, 25]
Dimensional Accuracy	±0.3–0.5% of net shape	±0.01 mm achievable	[23, 24]
Geometric Complexity	Excellent; net-shape, complex internal cavities possible	Limited by tool access and fixturing	[13]
Surface Oxidation Risk	High unless inert gas (argon) or vacuum used	Minimal if coolant/lubricant used properly	[19, 25]
Post-processing Needs	Debinding, sintering, optional surface treatment	Deburring, surface finishing, optional coating	[5]
Material Waste	Low (<5%)	High (40–70%)	[9, 12]
Cost Efficiency (High Volume)	Very high; tooling cost amortized over 10,000+ units	High cost per unit for small parts; low scalability	[10, 11]
Suitability for Medical Parts	Excellent; proven for implants and tools with biocompatibility	Excellent; widely used for prototypes and precision parts	[13, 21]

Based on previous studies and the advantages of MIM in producing various components, this study examines the feasibility of manufacturing a laparoscopic stapler joint using this process. A solution for manufacturing this product was proposed for the medical equipment industry. To achieve this, metal powder was first mixed with a polymer and injected into a mold, followed by debinding and sintering processes to produce the final part. The mechanical properties and dimensional accuracy of the manufactured product were then compared to a reference sample to assess its quality.

Methodology

This paper aims the feasibility study of manufacturing a laparoscopic stapler joint, which connects the housing and loading sections of the stapler. The mechanical properties and dimensional specifications of the MIM-produced part must match those of the reference component, which is manufactured by the Medtronic company under the Covidien brand. Figure 1 shows the laparoscopic joint reference part. The elemental analysis of the part is presented in Table 2. Based on the elemental composition, the part is made of 17-4PH stainless steel, a precipitation-hardening martensitic alloy known for its high strength and hardness after appropriate heat treatment. Three MIM samples were fabricated, and hardness was measured at three different locations on each sample. The average value of the three measurements was calculated for each sample and reported in Table 3. Hardness testing was conducted using the Vickers microhardness method (ASTM E384), with a load of 200 g and a dwell time of 15 seconds. The part was modeled using optical measurement tools, and microscopes, followed by the extraction of a 2D technical drawing. The manufactured part must meet specified dimensional tolerances. Dimensional inspection was conducted using optical measurement techniques and point cloud analysis with InnovMetric PolyWorks Metrology Suite 2022 software.

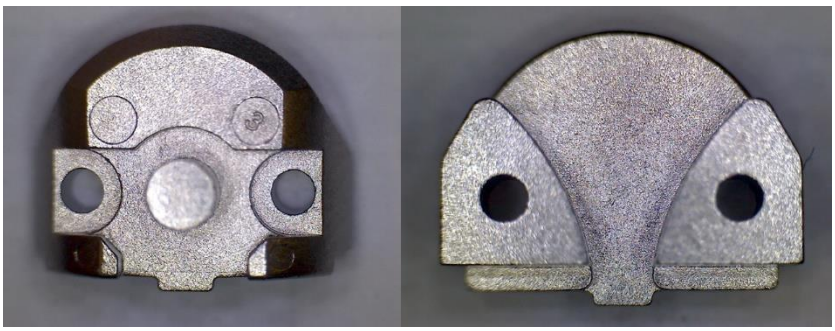

Figure 1. View of the laparoscopic joint component

Table 2. Elemental analysis of the covidien joint

Element	Wt. (ppm)
Cr	162000
Ni	46800
Cu	37200
Si	5700
Mn	3400
S	< 0.1
P	< 0.1

Table 3. Hardness measurement of samples

Sample 1	Sample 2	Sample 3
278 Hv	283 Hv	282 Hv

The feedstock specifically designed for the MIM process was sourced from Changsha Tijo Metal Material, a Chinese manufacturer, for the production of the laparoscopic stapler joint [26]. The mold was fabricated using milling and electrical discharge machining (EDM) techniques and was made from 1.2312 steel. To determine the appropriate shrinkage factor for the stapler joint, the part's geometry was analyzed. Since the part's walls are relatively simple, the shrinkage is uniform in all three dimensions. Based on the feedstock datasheet and screening tests, a material shrinkage rate of 16.5% was considered. The injection temperature was set between 170°C and 185°C, while the injection pressure was maintained between 50 and 80 bar. A catalytic debinding method was selected for binder removal, and a combination of solvent and thermal debinding was applied. Distilled water was used as the solvent, and the part was immersed in the solvent for four hours. After the solvent debinding stage, thermal debinding was conducted in a furnace at 150°C for approximately three hours, following the material datasheet specifications. It is important to note that the same furnace used for debinding was also used for sintering to minimize handling and prevent accidental damage to the part during transfer. Based on the provided details and material datasheet recommendations, sintering was performed at a temperature range of 1250–1300°C for approximately two hours. Due to the high operating temperature of the furnace, the support material used for holding the part was ceramic (Al_2O_3), as specified in the datasheet. Given the relatively simple geometry of the part and based on the screening tests, the specimens were positioned on one side during the heat treatment process (figure 2).

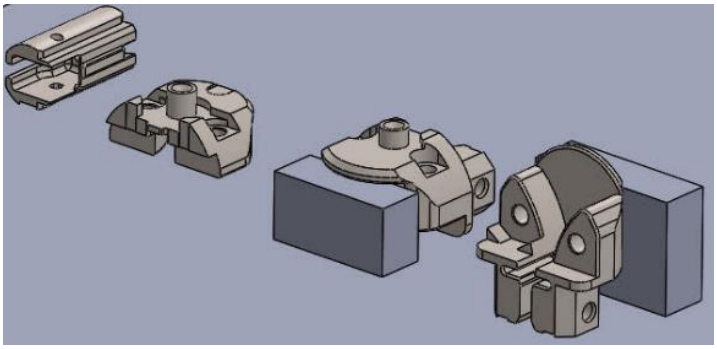

Figure 2. Suggested arrangement of stapler components in the furnace

Result and discussion

Examination of the manufactured part

The laparoscopic stapler joint was fabricated in a laboratory setting according to the described procedures and compared to the benchmark part (Figure 3 & figure 4). Various studies have used different criteria for evaluating and inspecting fabricated components. However, as previously mentioned, in this study, the manufactured part was evaluated based on three key aspects: material composition, hardness, and geometry, ensuring compliance with the established criteria. To verify the material composition, the manufactured part underwent XRD and elemental analysis (Table 4). Accordingly, the elemental composition confirmed that the material is the same as the 17-4PH, meeting the required standard. The hardness of the part was also measured, indicating a hardness of 306 Hv.

Additionally, the manufactured part was optically analyzed. After performing the optical inspection, the part was evaluated using InnovMetric PolyWorks, comparing it against the reference design and tolerance specifications. The analysis are illustrated in figure 5. As shown, nearly all of the part's features fall within the dimensional and geometric tolerances of the reference drawing. Dimensional tolerances were assessed against ISO 2768 standards and verified for functional compatibility with the design specifications of the laparoscopic stapler assembly. Two features were slightly out of tolerance; however, given the minimal deviation, they can be attributed to optical measurement errors, point-cloud mapping inaccuracies in the software, or similar factors, and thus can be disregarded. Finally, a comprehensive comparison of the part and the model was performed using a Color Map analysis. Based on the presented findings, it can be concluded that the manufactured part meets the geometric criteria set by the reference component.

Figure 3. Different views of the manufactured part using MIM

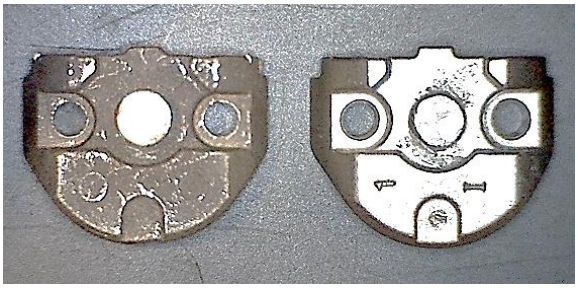

Figure 4. Visual comparison of the manufactured and benchmark part

Table 4. Elemental analysis of the manufactured part

Element	Wt. %
Al	0.294
Cr	15.677
Cu	4.031
Fe	74.433
Mg	0.159
Mn	0.411
Nb	0.275
Ni	3.815
P	0.017
S	0.169
Si	0.719

Object Name	Control	Nom	Meas	Tol	Dev	Test	Out Tol
cylinder 4	Radius	6.100	5.199	±1.000	-0.901	Pass	
circle 1	Diameter	2.400	1.750	±1.000	-0.650	Pass	
distance 5	3D Distance	2.800	2.431	±0.500	-0.369	Pass	
distance 12	3D Distance	2.800	2.611	±0.200	-0.189	Pass	
distance 4	3D Distance	2.050	1.879	±0.500	-0.171	Pass	
datum pattern C	2X Ø 1.600±0.170 mating	1.600	1.455	±0.170	-0.145	Pass	
cylinder 1	Radius	10.000	9.915	±0.220	-0.085	Pass	
cylinder 5	Radius	0.200	0.163	±0.050	-0.037	Pass	
distance 7	3D Distance	4.400	4.389	±0.050	-0.011	Pass	
circle 1	X	0.000	0.000	±1.000	0.000	Pass	
circle 1	Y	-3.650	-3.644	±1.000	0.006	Pass	
distance 8	3D Distance	5.650	5.661	±0.050	0.011	Pass	
cylinder 6	Radius	2.350	2.400	±0.080	0.050	Pass	
distance 3	3D Distance	1.000	1.068	±0.090	0.068	Pass	
distance 2	3D Distance	0.900	0.978	±0.080	0.078	Pass	
distance 6	3D Distance	3.350	3.439	±0.090	0.089	Pass	
distance 13	3D Distance	11.800	11.901	±1.000	0.101	Pass	
circle 1	Z	-7.600	-7.493	±1.000	0.107	Pass	
datum cylinder D	⌖ Ø 0.120 A B C		0.114	0.120	0.114	Pass	
distance 10	3D Distance	0.200	0.339	±0.150	0.139	Pass	
datum plane B	⊥ 0.150 A		0.151	0.150	0.151	Fail	0.001
datum plane A	▱ 0.150		0.159	0.150	0.159	Fail	0.009
datum pattern C	⌖ Ø 0.150 Ⓜ A B		0.161	0.189 (B: 0.039)	0.161	Pass	
datum cylinder D	Diameter	2.400	2.574	±0.180	0.174	Pass	
cylinder 2	Radius	5.400	5.640	±0.350	0.240	Pass	
plane 1	⌓ 0.700 Ⓤ 0.300 A B D		0.462	0.700	0.462	Pass	
distance 9	3D Distance	1.200	1.693	±0.500	0.493	Pass	
plane 2	⌓ 0.700 Ⓤ 0.300 A B D		0.617	0.700	0.617	Pass	

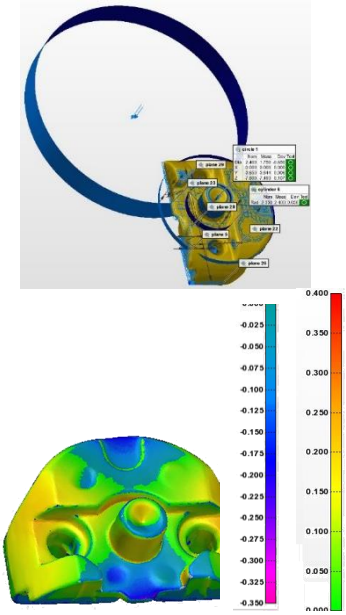

Figure 5. Tolerance inspection of the part in InnovMetric PolyWorks software

Optimization of Manufacturing Parameters

As seen in figure 6, the surface quality of the manufactured part is not in an optimal condition and has undergone oxidation. Given the medical application of this component, ensuring high surface quality is of critical importance. The oxidation occurred due to the reaction of the part with oxygen during the sintering process. To address this issue, an optimization approach was proposed by repeating the process using argon as a protective gas, considering its superior properties [25]. The part was re-manufactured under these revised conditions (Figure 6). As observed, the surface quality significantly improved, achieving the desired standard. The final component produced through this process was recorded as the finalized version. Additionally, given the nature of the optimized process, the manufacturing steps can be scaled up for industrial production and high-volume manufacturing.

Figure 6. Manufactured samples processed with protective argon gas.

Conclusion

The manufacturing of the laparoscopic stapler joint, given its complexities, presents significant challenges. In this study, a technically and economically viable manufacturing approach was proposed to overcome these challenges and offer a practical solution for the medical device industry. For producing components such as the laparoscopic stapler joint, two competing manufacturing methods exist: CNC machining and MIM. As demonstrated in this study, the mechanical properties of the MIM-manufactured part (specifically hardness) reached and even exceeded the desired values. Therefore, MIM can compete with CNC machining in terms of mechanical performance. The dimensional accuracy was also in acceptable range making the MIM as an optimal manufacturing method. It meets both mechanical and industrial requirements efficiently.

Disclosure statement and funding

The authors declare no potential conflicts of interest. The present study received no financial support from any organization or institution.

References

[1] Dadgar Asl, Y., Hassanzadeh, E., Akbari, M., Rahimi Asiabaraki, H., & Esfandiar, M. (2024). Investigating the Effects of Tool Pin Profile on Strain and Temperature During Friction Stir Welding Process Using CEL Method. *Journal of Engineering and Applied Research*, *1*(2), 213-223. https://doi.org/10.48301/jear.2024.473772.1037

[2] Zeinolabedin-Beygi, A., Naeini, H. M., Talebi-Ghadikolaee, H., Rabiee, A. H., & Hajiahmadi, S. (2024). Predictive modeling of spring-back in pre-punched sheet roll forming using machine learning. *The Journal of Strain Analysis for Engineering Design*, *59*(7), 463-474. https://doi.org/10.1177/03093247241263685

[3] Vijayan, S., Chelladurai, S. J. S., & Saiyathibrahim, A. (2024). Investigation on mechanical behavior of LM26 aluminum alloy—ZrB2 and copper-coated short steel fiber-

reinforced composites using stir casting process. *International Journal of Metalcasting*, 1-14. https://doi.org/10.1007/s40962-024-01303-x

[4] Rasti, A., Tarshizi, M., & Zeinolabedin-Beygi, A. (2024). Study of surface roughness, texture, and dimensional accuracy in thread whirling of Ti6Al4V screw. *Iranian Journal of Manufacturing Engineering*, *11*(4), 1-12. https://doi.org/10.22034/ijme.2024.460623.1966

[5] Ding, X.-P., Wang, C.-Y., Ruan, F.-J., Huang, Z.-P., Xu, W.-N., Luo, L.-M., Zan, X., & Wu, Y.-C. (2024). Formation mechanism of W-coated Cu composite powders and the metal injection molding using polyoxymethylene-based binders. *journal of materials research and technology*, *31*, 338-350. https://doi.org/10.1016/j.jmrt.2024.06.086

[6] Park, Y. A., Park, Y.-H., Ahn, M.-Y., & Yoon, Y. S. (2024). Fabrication and characteristics of Li2TiO3 pebbles manufactured by using powder injection molding (PIM) process. *Journal of Nuclear Materials*, *597*, 155140. https://doi.org/10.1016/j.jnucmat.2024.155140

[7] Fu, Y., Chen, M., Zou, H., Xiong, H., Kang, X., Zhang, L., & Zhou, K. (2024). Towards high-density and thick-walled NiFe2O4-based cermet by ceramic injection molding using spherical composite powder. *Ceramics International*, *50*(22), 46705-46717. https://doi.org/10.1016/j.ceramint.2024.09.022

[8] Falah, E. N., Pratiwi, V. M., Adityawan, I., Safrida, N., Wikandari, E., Widiyanto, A. R., & Abdullah, R. (2024). Research progress, potentials, and challenges of copper composite for metal injection moulding feedstock. *Powder Technology*, 119785. https://doi.org/10.1016/j.powtec.2024.119785

[9] Choi, S., Park, D., Lee, S., Song, M., & Kim, N. (2025). Prediction Model for Flake Line Defects in Metallic Injection Molding: Considering Skin-Core Velocity and Alignment. *Polymers*, *17*(2), 245. https://doi.org/10.3390/polym17020245

[10] Tadi, S. P., Koppisetti, D., Palisetti, V. K. T., Palivela, B. C., & Mamilla, R. S. (2025). Polymer based binder materials for various metal injection molding processes: Salient aspects and recent trends. *Journal of manufacturing processes*, *133*, 322-353. https://doi.org/10.1016/j.jmapro.2024.11.032

[11] Bahanan, W., Fatimah, S., Song, H., Lee, E. H., Kim, D.-J., Yang, H. W., Woo, C. H., Ryu, J., Widiantara, I. P., & Ko, Y. G. (2023). Moldflow Simulation and Characterization of Pure Copper Fabricated via Metal Injection Molding. *Materials*, *16*(15), 5252. https://doi.org/10.3390/ma16155252

[12] Meza, A., Barbosa, A., Tabares, E., & Torralba, J. M. (2024). Tailoring high-entropy alloys via commodity powders for metal injection moulding: A feasibility study. journal of materials research and technology, 31, 109-116. https://doi.org/10.1016/j.jmrt.2024.06.034

[13] Dehghan-Manshadi, A., Yu, P., Dargusch, M., StJohn, D., & Qian, M. (2020). Metal injection moulding of surgical tools, biomaterials and medical devices: A review. *Powder Technology*, *364*, 189-204. https://doi.org/10.1016/j.powtec.2020.01.073

[14] Hamidi, M. F. F. A., Harun, W. S. W., Samykano, M., Ghani, S. A. C., Ghazalli, Z., Ahmad, F., & Sulong, A. B. (2017). A review of biocompatible metal injection moulding

process parameters for biomedical applications. *Materials Science and Engineering: C*, *78*, 1263-1276. https://doi.org/10.1016/j.msec.2017.05.016

[15] Kultamaa, M., Mönkkönen, K., Saarinen, J. J., & Suvanto, M. (2022). Self-lubrication of porous metal injection molded (MIM) 17-4PH stainless steel by impregnated paraffin wax. *Tribology International*, *174*, 107735. https://doi.org/10.1016/j.triboint.2022.107735

[16] Reclaru, L., Ionescu, F., & Diologent, F. (2024). Evaluation of the Corrosion Resistance of Watch Links from 316L and 904L Austenitic Stainless Steels Obtained by the Metal Injection Molding (MIM) Technique Intended to Be in Contact with Human Skin. *Coatings*, *14*(4), 412. https://doi.org/10.3390/coatings14040412

[17] Noraphaiphipaksa, N., Manonukul, A., Kanchanomai, C., & Mutoh, Y. (2024). Fretting fatigue behavior of metal injection molded stainless steel MIM 316L with small pores and low porosity. *Tribology International*, *193*, 109332. https://doi.org/10.1016/j.triboint.2024.109332

[18] Lin, K.-H. (2011). Wear behavior and mechanical performance of metal injection molded Fe–2Ni sintered components. *Materials & Design*, *32*(3), 1273-1282. https://doi.org/10.1016/j.matdes.2010.09.034

[19] Shieddieque, A. D., Virdhian, S., Muttahar, M. I. Z., & Muttaqin, M. R. (2021). Effects of sintering variables on the physical and mechanical properties of metal injection molding molded 17-4 ph stainless steel. Materials Science Forum,

https://doi.org/10.4028/www.scientific.net/MSF.1028.403

[20] Panahizadeh, V., Khorsand, H., & Azadeh, M. (2021). The Numerical and Experimental Investigations of Injection Mold Filling and Determination of the Appropriate Conditions in Metal Injection Molding (MIM). *Aerospace Mechanics, 17(3),* 97-112. (in Persian) DOR: 20.1001.1.26455323.1400.17.3.8.3

[21] Hamidi, M., Harun, W., Khalil, N., Ghani, S., & Azir, M. (2017). Study of solvent debinding parameters for metal injection moulded 316L stainless steel. IOP Conference Series: Materials Science and Engineering, https://doi.org/10.1088/1757-899X/257/1/012035

[22] Momeni, V., & Alaei, M. (2019). Optimization of injection parameters in metal injection molding of 4605 low alloy steel. *Modares Mechanical Engineering*, *19*(5), 1199-1208. (in Persian) DOR: 20.1001.1.10275940.1398.19.5.23.5

[23] Rezaei, S., & Askari, A. (2024). Investigating metal injection molding of AISI-4605 low alloy steel feedstock: parametric optimization of the injection stage using RSM technique. *Iranian Journal of Manufacturing Engineering*, *11*(3), 13-25. (in Persian) https://doi.org/10.22034/ijme.2024.440630.1926

[24] Yang, S., Zhang, R., & Qu, X. (2015). Optimization and evaluation of metal injection molding by using X-ray tomography. *Materials Characterization*, *104*, 107-115. https://doi.org/10.1016/j.matchar.2015.04.014

[25] Langlais, D., Demers, V., & Brailovski, V. (2022). Rheology of dry powders and metal injection molding feedstocks formulated on their base. *Powder Technology*, *396*, 13-26. https://doi.org/10.1016/j.powtec.2021.10.039

[26] Hwang, I.-S., So, T.-Y., Lee, D.-H., & Shin, C.-S. (2023). Characterization of mechanical properties and grain size of stainless steel 316L via metal powder injection molding. *Materials*, *16*(6), 2144. https://doi.org/10.3390/ma16062144